EPJ Web of Conferences **3**, 07014 (2010)
DOI:10.1051/epjconf/20100307014

The investigation of $\Lambda(1405)$ state in the stopped K^- reaction on deuterium

T. Suzuki[1,a], J. Esmaili[2,3], and Y. Akaishi[2,4]

[1] Department of Physics, The University of Tokyo, Tokyo 113-0033, Japan
[2] RIKEN Nishina Center, RIKEN, Saitama 351-0198, Japan
[3] Department of Physics, Isfahan University of Technology, Isfahan 84156-83111, Iran
[4] College of Science and Technology, Nihon University, Chiba 274-8501, Japan

Abstract. Nowadays, extensive studies of the problem of the deeply bound $\bar{K}$ nuclei stimulate the reconsideration of $\Lambda(1405)$ state as the theoretical basis of the binding of $\bar{K}$ nuclei, and the old question of the nature of $\Lambda(1405)$ becomes a modern subject by the new interest. In contrast to one of conventional interpretations of $\Lambda(1405)$ as the $\bar{K}N$ quasi-bound state at 1405 MeV/c^2, a two-pole hypothesis, by which $\Lambda(1405)$ consists of two poles at 1420 and 1390 MeV/c^2 couple mainly with $\bar{K}N$ and $\Sigma\pi$ channels, respectively, was proposed recently. On the other hand, a very recent theoretical analysis has clarified that the $(\Sigma\pi)^0$ invariant mass spectra after K^- absorption in d reflect strikingly resonant formation of $\Lambda(1405)$ (or $\Lambda(1420)$) and thus are capable of distinguishing different Ansatz's. We have proposed a new experiment by means of the stopped K^- reaction on liquid deuterium at J-PARC K1.8BR beamline with E15/E17 experimental devices, so as to give a new precision- and high-statistics-data of $(\Sigma\pi)^0$ mass spectra to examine the issue, $\Lambda(1405)$ or $\Lambda(1420)$, in the most reliable way, and thus to answer the most fundamental questions of $\bar{K}N$ interaction and $\bar{K}$ nuclei.

1 Physics motivation

$\Lambda(1405)$ was discovered in 1961 as a broad peak in the $(\Sigma\pi)^0$ invariant mass spectrum from the $K^-p \to (\Sigma\pi)^0 + (\pi\pi)^0$ reaction measured in a hydrogen bubble chamber exposed to the 1.15 GeV/c K^- beam [1], and was attributed to a baryon species with strangeness $S = -1$, spin-parity $J^P = (1/2)^-$, and isospin $I = 0$. While its assignment to an ordinary 3-quark state is difficult, it has been interpreted as a quasi-bound state of K^-p. At the end of the last century the so called anti-kaonic hydrogen puzzle was resolved by a KEK-PS E228 experiment [2], indicating that $\Lambda(1405)$ is most likely to be a strongly bound K^-p state. Triggered by the experimental result, Akaishi and Yamazaki postulated $\Lambda(1405)$ as an $I = 0$ $\bar{K}N$ bound state, and constructed the $\bar{K}N$ interaction so as to reproduce the mass and width of $\Lambda(1405)$ and the low energy $\bar{K}N$ scattering data [3]. Furthermore, they applied this very attractive phenomenological interaction to few-nucleon systems involving a $\bar{K}$, and predicted deeply bound discrete $\bar{K}$ nuclear states with unusually high nuclear densities [4] [5].

According to the prediction, many search experiments were performed from the early 2000s, and new experimental plans are now in progress in the world. Some of these groups reported possible candidates of $\bar{K}$ bound systems, and intensive discussions are being developed, not only experimentally but also theoretically. In contrast to the Akaishi-Yamazaki's interpretation of $\Lambda(1405)$, a double-pole hypothesis claims that $\Lambda(1405)$ consists of two poles at 1420 and 1390 MeV/c^2, which are coupled mainly to $\bar{K}N$ and $\Sigma\pi$ channels, respectively. Then, the less attractive $\bar{K}N$ interaction leads to shallower binding of $\bar{K}$ nuclei, as claimed by several authors [6] [7]. Concerning the mass and width of $\Lambda(1405)$ a question can also be casted to the current PDG[1] values of the mass and the width of $\Lambda(1405)$, which were adopted from Dalitz-Deloff's analysis [8] of $K^-p \to \Sigma^+(1660)\pi^-$ data at $p_{K^-} = 4.2$ GeV/c on a hydrogen bubble chamber [9]. Thus, the present knowledge about $\Lambda(1405)$, the most important basic building block of kaonic nuclear systems, remains highly controversial, and the current issue, $\Lambda(1405)$ or $\Lambda(1420)$, should be discriminated experimentally.

2 Λ^* problem and $\bar{K}N \to \Sigma\pi$ reaction

The problem of $\Lambda^*(\equiv \Lambda(1405)$ or $\Lambda(1420))$ is the most clearly illustrated in the difference of $\bar{K}N$ scattering length between counter hypothesis. The figure 1 exhibits a comparison of isospin $I = 0$ $\bar{K}N$ scattering amplitudes between calculations by chiral-SU(3) ($\Lambda(1420)$: double-pole) [7] and phenomenology ($\Lambda(1405)$:single-pole) [4]. In the former calculation, imaginary part of the amplitude does not show any bump structure by the second pole. This phenomenon, which is commonly shown by many calculations based on the chiral SU(3) dynamics, indicates no effect of the second pole in the $\Sigma\pi \to \Sigma\pi$ channel to the $\bar{K}N \to \Sigma\pi$ invariant mass spectrum, because the imaginary part is directly connected to the spectrum as discussed right after.

[a] e-mail: tsuzuki@phys.s.u-tokyo.ac.jp

[1] Particle Data Group.

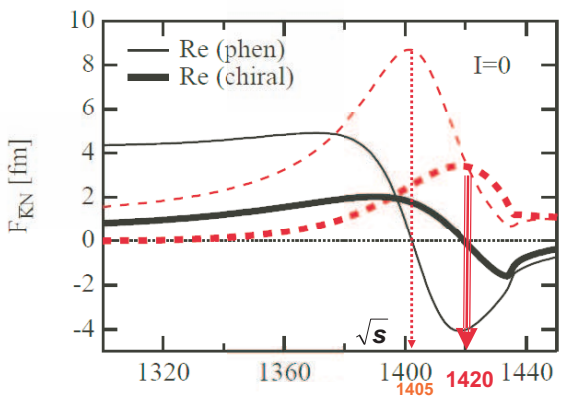

Fig. 1. A comparison of $\bar{K}N$ scattering amplitudes between counter models. The red dashed curves are imaginary parts, while black real ones are real parts. Thin and thick lines represent phenomenological [4] and Chiral SU(3) [7] models, respectively.

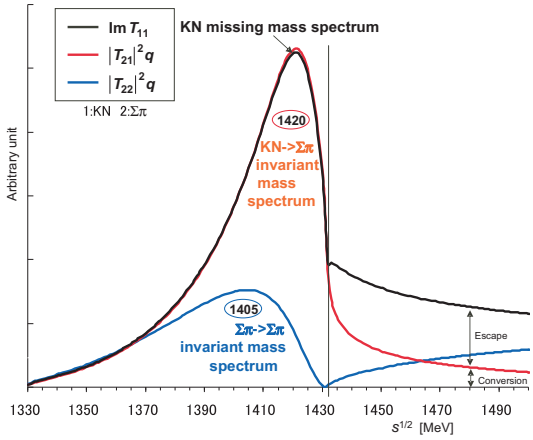

Fig. 2. T-matrix elements and experimental observables.

Figure 2 shows the relationship between T-matrix elements and experimental observables. The T-matrix elements are calculated from Hyodo-Weise's Chiral SU(3) dynamics [7], for which pole positions are

$$z_1\ (\bar{K}N - \Sigma\pi) : 1432 - 17i\ \text{MeV}, \quad (1)$$
$$z_2\ (\Sigma\pi - \Sigma\pi) : 1398 - 73i\ \text{MeV}. \quad (2)$$

The imaginary part of the scattering amplitude shown in the figure 1 is proportional to the Im T_{11} drawn here by black solid curve. This coincides with $\bar{K}N \to \Sigma\pi$ invariant mass spectrum, $|T_{21}|^2 \cdot q$, in the $\bar{K}N$ bound region. Namely,

$$Im(F_{\bar{K}N}) \propto Im(T_{11}) = |T_{21}|^2 \cdot q, \quad (3)$$

and hence the $\bar{K}N \to \Sigma\pi$ invariant mass spectrum is just proportional to the imaginary part of the $\bar{K}N$ scattering amplitude, to which no $\Sigma\pi \to \Sigma\pi$ second pole effect is expected according to the figure 1. Furthermore, it should be noted here that the second pole is the object described by T_{22}, and only sensitive to the $\Sigma\pi \to \Sigma\pi$ elastic scattering. Therefore, the observation of $\bar{K}N \to \Sigma\pi$ invariant mass spectrum directly lead the imaginary part of the I=0 $\bar{K}N$ scattering amplitude which is the focal point of the present physics discussion, and the spectrum depends exclusively on the first or single pole position, regardless the presence or position of the second pole. The availability of the $\bar{K}N \to \Sigma\pi$ reaction to determine the first pole position is also pointed out by the chiral unitary approach [10].

3 $K^-_{stopped} d \to (\Sigma\pi)^0$ reaction

Although the validity of the $\bar{K}N \to \Sigma\pi$ reaction to study Λ^* has been verified, the direct production of Λ^* in the $\bar{K}N \to \Sigma\pi$ reaction is kinematically forbidden due to its sub-threshold feature, and we do need to consider nuclear targets to take energy away from initial kaon. From this viewpoint, a possibility of $K^- d \to \pi\Sigma n$ reaction in kaon in-flight kinematics, in which nuclear Auger process predominantly occurs (figure 3), has been discussed by several authors [10], and corresponding experiment has been proposed [11]. On the other hand, a very recent theoretical analysis [12] has clarified that the $(\Sigma\pi)^0$ invariant mass spectra after K^- absorption in ^{4}He, ^{3}He and d do reflect resonant formation of $\Lambda(1405)$ (or $\Lambda(1420)$) via the spectator process by the projection onto well-known Fermi momentum distribution in the target nuclei, and the mass and width of $\Lambda(1405)$ have been actually determined to be $Mc^2 = 1405.5^{+1.4}_{-1}$ MeV and $\Gamma = 26^{+4}_{-3}$ MeV from a statistical analysis of an old bubble chamber data on ^{4}He [13]. Furthermore, it was pointed out that the target of d, as the calculated spectra are shown in figure 4, is even more interesting, because the "quasi-free" shape of $M_{(\Sigma\pi)^0}$ is narrow enough because of the low internal momentum of the spectator n to observe a resonant $\Lambda(1405)$ as a separate peak on a distant tail which is expected from the high-Fermi-momentum component of realistic deuteron wave function [14].

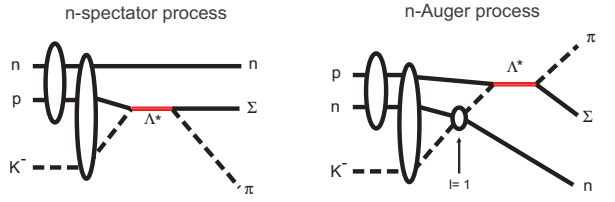

Fig. 3. Diagrams for the neutron-spectator and the nuclear Auger processes of the $K^- d \to \pi\Sigma n$ reaction [14]. The former process dominates the reaction for a lower incident K^- momentum, while the latter dominates for a higher incident K^- momentum [10] [14].

Figure 5 shows $d(K^-_{stopped}, n)(\Sigma\pi)^0$ spectrum calculated from various published $\bar{K}N$ scattering amplitudes [7] [15] in a model-independent way with realistic Fermi momentum distribution. As it is expected from the discussion de-

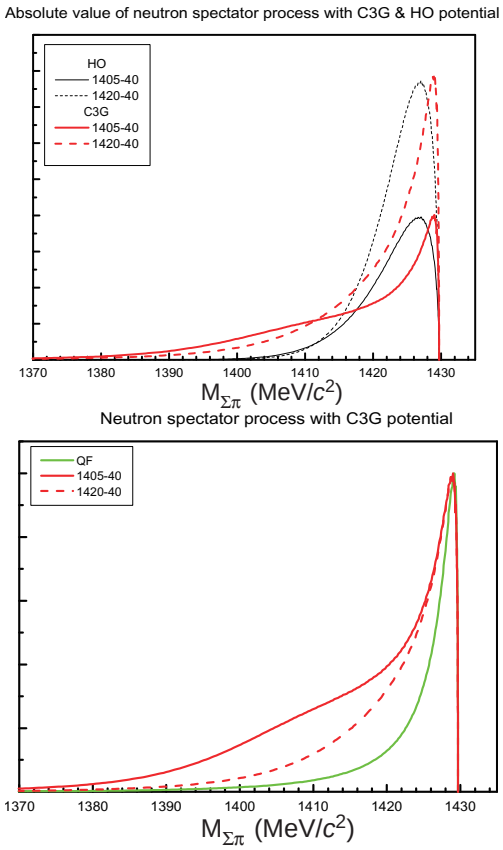

Fig. 4. Top: $M_{(\Sigma\pi)^0}$ spectra calculated with harmonic oscillator (black) and realistic (red) deuteron wave functions. The solid and dashed lines are results from M_{Λ^*} = 1405 and 1420 (MeV/c^2), respectively. Bottom: Calculated $M_{(\Sigma\pi)^0}$ spectra compared by scaling each of spectra so as to adjust the peak values to be equal. The red solid- and dashed-lines represent the result of M_{Λ^*} = 1405 and 1420 (MeV/c^2), respectively, while the green solid line is the "quasi-free" spectrum shape.

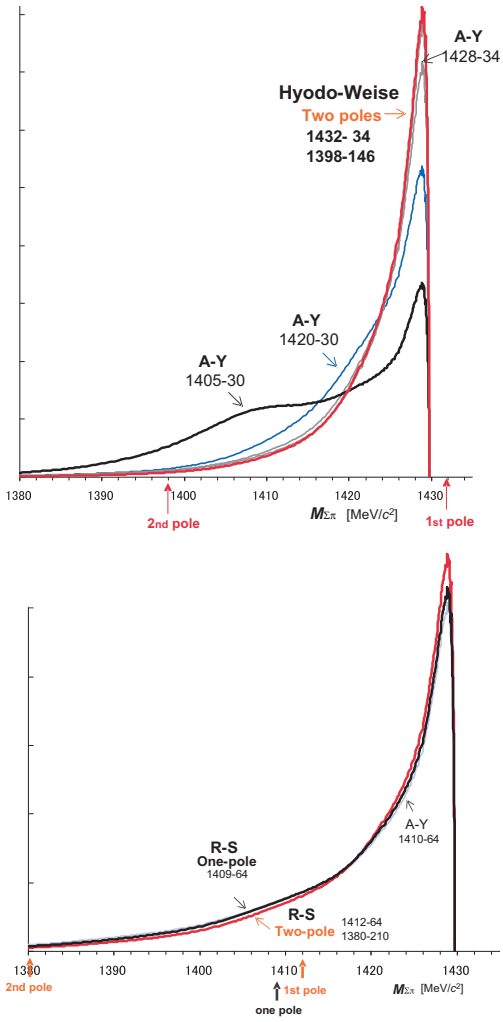

Fig. 5. Top: $(\Sigma\pi)^0$ invariant mass spectrum from stopped K^- reaction on d, calculated from two-pole model [7]. For the comparison, spectra calculated from single pole model with various pole positions are overlaid. Bottom: Spectra from same reaction from different model [15], and their comparison with single-pole model with similar pole position.

veloped in the previous section, the spectrum shape depends exclusively on the first/single pole position, and conversely, the pole position is uniquely and exactly derived from the spectrum shape. Thus, we propose the present experiment adopting $d(K^-_{stopped}, n)(\Sigma\pi)^0$ reaction, to examine the issue, $\Lambda(1405)$ or $\Lambda(1420)$, in the most reliable way.

4 Experimental Method

4.1 Principle of the measurement

In the experiment, we aim to measure the $(\Sigma\pi)^0$ mass spectra from the stopped K^- reaction on a deuterium target. In order to achieve a high mass resolution of $\Sigma^\pm\pi^\mp$ produced in the $\Sigma^\pm\pi^\mp n$ final states of the stopped K^- reaction on deuterium, we perform a missing mass spectroscopy of the neutron in coincidence with the charged pion,

$$K^-_{stopped} + d(\rightarrow \text{"}\Lambda(1405)\text{"} + n) \rightarrow \widetilde{\Sigma^\pm} + \pi^\mp_{primary} + n_{primary}, \quad (4)$$

where $\pi^\mp_{primary}$ and $n_{primary}$ are pion and neutron from the primary reaction detected in coincidence, and $\widetilde{\Sigma^\pm}$ denotes undetected $\Sigma^\pm$ particles in the final states. Then, the mass of $(\Sigma\pi)^0$ system, $M_{(\Sigma\pi)^0}$, is kinematically identified as the missing mass evaluated from the detected neutron momentum, $MM(n)$,

$$M_{(\Sigma\pi)^0} = MM(n) \equiv \sqrt{(M_{K^-} + M_d - E_n)^2 - (p_n)^2}, \quad (5)$$

where M_{K^-}, M_d, M_n denote the masses of K^-, d, and n, respectively, $\mathbf{p}_n$ is detected neutron 3-momentum, and $E_n = \sqrt{(M_n)^2 + (p_n)^2}$ is the neutron energy.

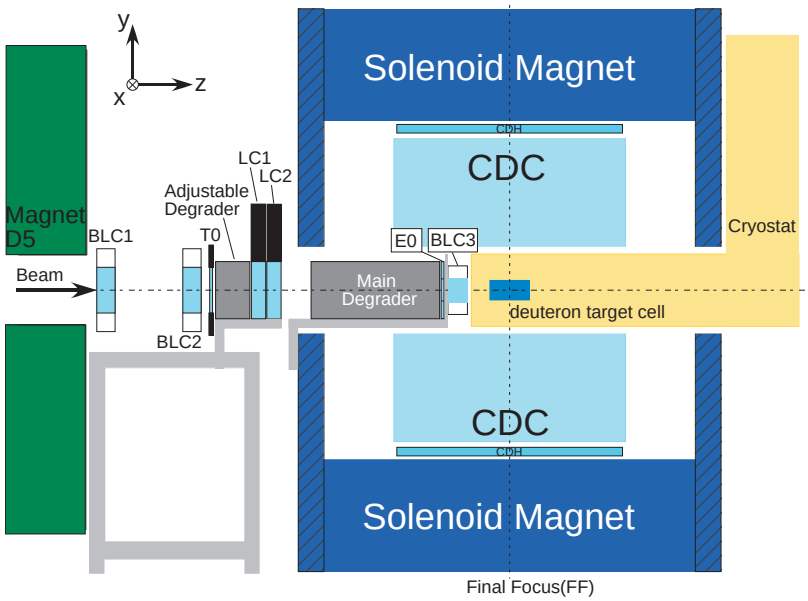

Fig. 6. A schematic view of the setup of the proposed experiment.

In addition, hyperon mass, $M_{Y^{\pm}}$, is reconstructed from the neutron and pion momenta, as

$$M_{Y^{\pm}} = \sqrt{(M_{K^-} + M_d - E_T)^2 - (p_T)^2}, \quad (6)$$

where $E_T = E_n + E_{\pi^{\mp}}$ and $\mathbf{p}_T = \mathbf{p}_n + \mathbf{p}_{\pi^{\mp}}$. Then, the requirement,

$$M_{Y^{\pm}} = M_{\Sigma^{\pm}}, \quad (7)$$

ensures the discrimination of the detected n and $\pi^{\mp}$ pair from wrong combinations with secondary $\pi^{\mp}$ and n from the weak decay of $\Sigma^{\pm}$, $\widetilde{\Sigma^{\mp}} \rightarrow n_{decay} + \pi^{\mp}_{decay}$, or the other hadronic reactions, and hence the equality, $M_{(\Sigma\pi)^0} = MM(n)$. Obviously, possible contaminants from in-flight K^-d reactions are also rejected. Actually, Λdn and $\Sigma^0 dn$ final states of stopped K^- reaction on ^{4}He, were successfully discrminated in KEK-PS E549 in this way [16].

4.2 Overview of the experiment

A schematic description of the experimental setup is given in figure 6. The setup, including the setting and the central momentum of K1.8BR beamline, is almost identical to that of E17 which is described in detail in the proposal [17] and the proceedings of this conference [18], [19]. Therefore, here we briefly describe the features specific to the proposed experiment [20].

1. **The target material.** Target material is replaced from liquid ^{3}He to deuterium, with the same container and cooling system.
2. **Removal of the E17 X-ray Detectors.** The Silicon Drift Detectors (SDD) placed in the cryostat surrounding the target cell for the X-ray detection are removed from E17 setup.
3. **CDS operation mode.** In the E17 experiment, CDS is used as a tracker of secondary charged particle just to get the reaction vertex without magnetic field. In the present experiment, a 0.5 T field is applied along the z-direction for momentum measurement, as in E15.
4. **E0 counter**. In the E17 experiment, E0, which is the counter located most downstream for incident kaon detection, is expected to supply pulse height information to select "stopped" K^- events. In the present experiment, it also gives the start timing of neutron TOF measurement.

In the experiment, we perform a coincidence measurement of a neutron and a charged pion. The neutron is detected by 3cm-thick plastic scintillators, CDH, and identified by using the CDC as VETO detector to separate charged particles. Then, the TOF of a neutron is measured as

$$TOF = T_{CDH} - T_{E0} - T_{E0->stop}, \quad (8)$$

where T_{CDH} is the time when a CDH is fired by the neutron, T_{E0} is the time of beam kaon arrival onto the E0 counter. and $T_{E0->stop}$ is kaon flight time from E0 arrival to its stop inside the target. Combined with the neutron hit position given by CDH and reaction vertex given by kaon and charged particle tracks measured by BLC3 and CDC, respectively, the TOF is converted into the neutron momentum. The momentum, charge, and species of secondary charged particles are identified by CDS, as described in the E15 proposal [21] and the proceedings of this conference [22].

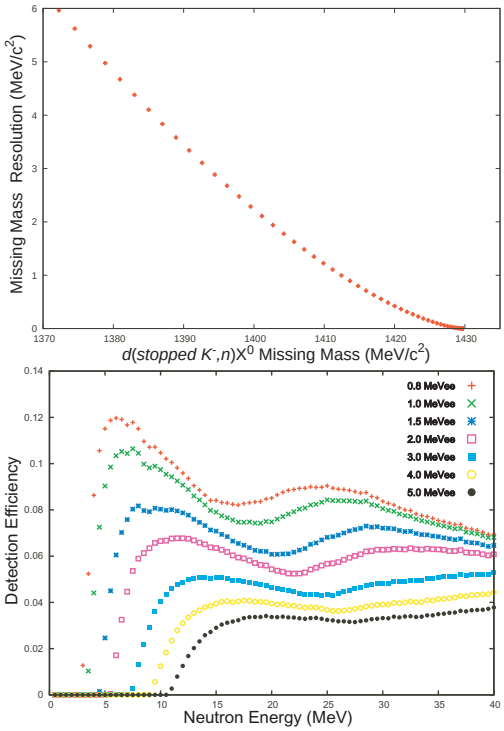

Fig. 7. Top: Calculated $M_{(\Sigma\pi)^0}$ resolution (σ) as the function of $M_{(\Sigma\pi)^0}$. Bottom: neutron detection efficiency of a CDH segment for various software detection thresholds, as the functions of neutron energy.

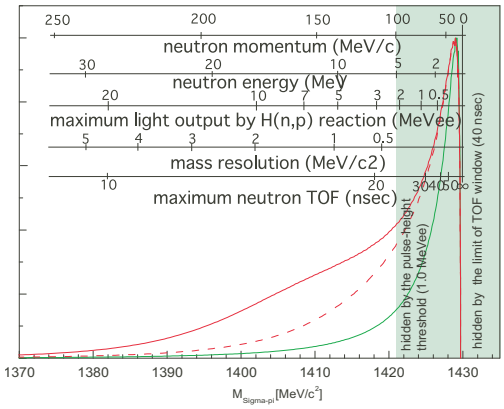

Fig. 8. Calculated spectra and mass-dependences of relevant quantities.

4.3 Neutron detection efficiency and $(\Sigma\pi)^0$ mass resolution

As already described, the neutron from the reaction is measured by a TOF method with a mean flight distance of ~60 cm. The mass resolution, which is conservatively estimated to be ~2 MeV at the most interesting region assuming a 400 psec TOF resolution as the achievement of KEK-PS E549 for 3 MeV*ee* γ-ray, is exhibited in the top of figure 7, as a function of missing mass. As the E17 trigger, electronics and DAQ systems have the time gate length up to ~ 40 nsec to CDH-detected particles, the minimum neutron energy in time for the timing gate is ~2 MeV, which defines an upper limit on the sensitive mass, 1427 MeV/c^2. Those neutrons are detected with 36 segments of 79cm-length, 10cm-wide, 3cm-thick scintillation counters, CDH, which are made of EJ200 plastic. The detection efficiency is quantitatively simulated by DEMONS (Differential Efficiency for Multi-cell Organic Neutron Scintillators) [23] as the function of neutron incident energy. The results obtained for various software thresholds with hardware (discriminator) threshold of 0.6 MeV*ee* and the light attenuation length of 329 cm are shown in the bottom of figure 7. It is found that sensitive neutron kinetic energy is over 5 MeV applying a 1.0 MeV*ee* software threshold, which defines an upper limit on the sensitive $M_{(\Sigma\pi)^0}$ of ~1421 MeV/c^2. In the present experiment, we aim to apply a 1.0 MeV*ee* software threshold to be sensitive up to ~ 1420 MeV/c^2.

In figure 8, calculated spectra are shown with the experimental conditions to summarize the situation.

4.4 Calibration method of neutron TOF

As is found in the $1/\beta_n$ spectrum from stopped K^- reaction on ^{4}He from KEK E549 experiment (figure 9),

1. γ-ray ($1/\beta_n$ = 1.0), and
2. neutron from $\Sigma^+_{stopped} \rightarrow n\pi^+$ ($1/\beta_n$=5.176)

are available for the calibration of TOF of neutral particles in the stopped K^- reaction. Accordingly, the calibration is robust by those two intense monochromatic peaks by γ and n, and neutron energy resolution is directly and exactly determined by neutron at the energy region of interest for this experiment. This is one of strong advantages of this experimental program, since neutron energy resolution is normally not exactly known at the interested energy range.

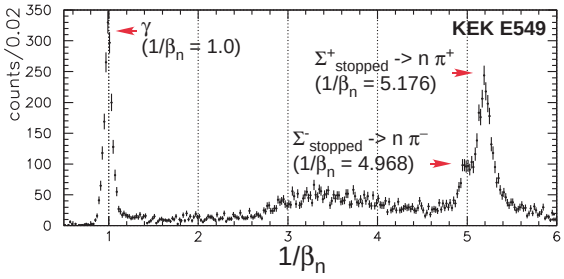

Fig. 9. $1/\beta$ spectrum for neutral particles from KEK-PS E549 experiment, under $n - \pi$ back-to-back event selection [24].

4.5 Identification of $\Sigma^{\pm}\pi^{\mp}n$ final states

Following the reaction,

$$K^-_{stopped} + d \rightarrow \Sigma^{\pm} + \pi^{\mp}_{primary} + n_{primary}, \qquad (9)$$

the $\Sigma^{\pm}$ can weakly decay into $n_{decay}+\pi^{\pm}_{decay}$. If n_{decay} and/or $\pi^{\pm}_{decay}$ are detected and combined, they produce combinatorial background in the $M_{Y^{\pm}}$ spectra. This synchronized

background is considered to be the most dominant one of our measurement, and it should be examined in advance together with the feasibility of identification of $\Sigma^{\pm}\pi^{\mp}n$ final states. In figure 10, simulated $M_{Y^{\pm}}$ spectra constructed from all combinations of detected $n\pi^{\pm}$ pairs are exhibited for $M(\text{"}\Lambda(1405)\text{"}) = M(\Sigma^{\pm}\pi^{\mp}) = 1400$ MeV/c^2. In the simulated spectra, $\Sigma^{\pm}$ appear as well isolated peaks, and $\Sigma^{\pm}\pi^{\mp}n$ final states are identified by S/N ratio better than 5.

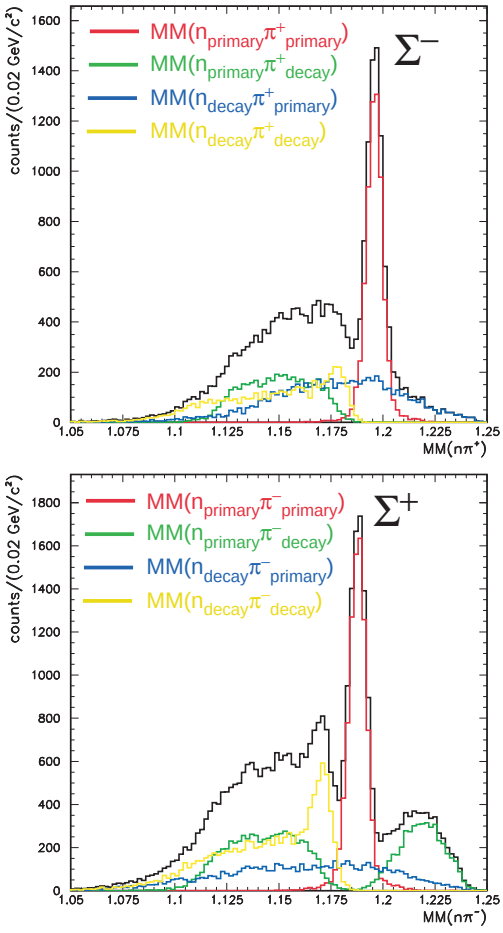

Fig. 10. Simulated $M_{Y^{\pm}}$ spectra from the reaction for $M_{(\Sigma\pi)^0} = 1.40$ GeV/c^2. Contributions from all four possible components are separately shown (colors) with overall spectra (black).

The following two facts should be noted here:

1. The $M_{Y^{\pm}} = MM(n\pi^{\mp})$ spectra depend on $M_{(\Sigma\pi)^0}$. Therefore, overall S/N ratio must depend on the global spectrum shape of $M_{(\Sigma\pi)^0}$.
2. Requiring a further coincidence detection of $\pi^{\pm}_{decay}$, further improvement of S/N ratio is possible, as contributions originate from n_{decay} (blue and yellow lines in the figure) can be eliminated by requiring the condition, $IM(n\pi^{\pm}) \neq M_{\Sigma^{\pm}}$, where $IM(n\pi^{\pm})$ is the invariant mass constructed by detected n and $\pi^{\pm}$.

4.6 Acceptance correction

For the coincidence measurement of $n\pi^{\pm}$ from the stopped K^- reaction, acceptance can be corrected in general by an acceptance function, $\epsilon_{n\pi^{\pm}}$, defined by three kinematical variables, p_n, $p_{\pi^{\pm}}$, and $\cos\theta \equiv \mathbf{p}_n \cdot \mathbf{p}_{\pi^{\pm}}/(p_n \times p_{\pi^{\pm}})$ in a process-independent way from the spherical symmetry of the reaction. Now, let us define the distribution function of these three variables, $\phi_{n\pi^{\pm}}$, from which any distribution of any dynamical variable of n and $\pi^{\pm}$ is derived, could be constructed as

$$\phi_{n\pi^{\pm}}(p_n, p_{\pi^{\pm}}, cos\theta) = \frac{C_{n\pi^{\pm}}(p_n, p_{\pi^{\pm}}, cos\theta)}{N_{stopK^-} \times \epsilon_{n\pi^{\pm}}(p_n, p_{\pi^{\pm}}, cos\theta)}, \quad (10)$$

where N_{stopK^-} is the total number of the stopped K^-, $C_{n\pi^{\pm}}(p_n, p_{\pi^{\pm}}, cos\theta)$ is the count number of each three dimensional bin. For three-body final states like $\Sigma^{\pm}\pi^{\mp}n$, the acceptance function is reduced to be defined only by p_n and $p_{\pi^{\pm}}$ under the kinematical constraint. Thanks to the spherical symmetry of CDS, the acceptance map can be exactly evaluated. The neutron efficiency is, as already described, estimated with DEMONS, to which the outputs are well examined and highly reliable in the neutron momentum region interested in the present experimental program.

5 Trigger, Rate and Yield Estimations

As the experiment is essentially the coincidence measurement of incident K^-, n, and $\pi^{\pm}$, the trigger scheme is the most simply represented as $\widehat{K^-} \otimes \widehat{CDH}$, where $\widehat{K^-}$ denotes incoming K^- identified by scintillation counters and Lucite Cherenkov counters located in the beam line, and $\widehat{CDH}$ denotes a hit on CDH.

In order to estimate the trigger rate, we refer to the KEK-PS E570, where the trigger scheme, $\widehat{K^-} \otimes (\widehat{TC} \oplus \widehat{PA} \otimes \widehat{PB})$, and the detector location were essentially identical to the present case with smaller solid angle coverage of TC⊕PA⊗PB(25 %) [17] compared to CDH (60 %). In both experiments, trigger rate is predominantly determined by, and is proportional to the product of *incident K^- number reached the last beamline counter*, $N^L_{K^-}$, which is nearly identical to the number of $\widehat{K^-}$, and the solid angle coverage for secondary particle detection, as the trigger number is actually dominated by in-flight decay of decelerated low-energy K^-. Now, we compare the *incident K^- number to the first beam counter*, $N^f_{K^-}$, between two experiments. In the present program, $N^f_{K^-}$ is estimated as ~10k events per spill by TURTLE simulation assuming 27kW-equivalent primary beam power and present K1.8 beamline, while $N^f_{K^-}$ at KEK-PS K5 is known to be ~20k for 2×10^{12} ppp as an achievement of KEK 12 GeV PS for E570. Here let we assume that the $N^L_{K^-}/N^f_{K^-}$ ratio, which represents the survival rate of K^- during its deceleration within degraders, are identical to both experiments. Then,

the ratio of trigger number per spill (N_{trg}) in the two experiments, are evaluated as

$$\frac{N_{trg}(\text{present})}{N_{trg}(\text{E570})} = \frac{\frac{N^L_{K^-}}{N^f_{K^-}} \times N^f_{K^-}(\text{present})}{\frac{N^L_{K^-}}{N^f_{K^-}} \times N^f_{K^-}(\text{E570})} \times \frac{\Omega(CDH)}{\Omega(TC \oplus PA \otimes PB)} = 1.2. \quad (11)$$

Accordingly, the actual rate in the present program is then estimated to be

$$1.2 \times 550(\text{E570 result}) \times \frac{1.6(\text{FT duration of KEK PS})}{0.7(\text{of J-PARC PS})} \sim 1.5\text{k (events)/s}. \quad (12)$$

Since we will actually request hit multiplicity≥2 for $\widehat{CDH}$, the trigger rate will drastically decrease relative to the estimation above, because the multiplicity ≥ 2 condition eliminates >90% of the in-flight K^- decays, which contributed dominantly to the E570 trigger rate. Therefore, the moderate and controllable value, 1.5 k(events)/s, is the absolute upper limit of the trigger rate of the experiment.

Now, let us switch the discussion to the yield estimation. Here we denote expected modes with lower suffix i, ($i = 1, 2, ...$). Expected yield of $\Sigma^-\pi^+n$ (mode 1) and $\Sigma^+\pi^-n$ (mode 2) events, Y_i, are estimated from the following relationship,

$$Y_i = N_{stoppedK^-} \times Br_i \times \epsilon_\pi \times \epsilon_n \times \epsilon_{DAQ} \times \epsilon_{ANA}, \quad (13)$$

where

$N_{stoppedK^-}$: total number of stopped $K^- = 1.9\times10^7$, which will be achieved in 14 days with 27kW-equivalent primary beam intensity at present K1.8BR beamline,
Br_i : branching ratio to the $i-th$ mode, 0.22 and 0.30 for $i = 1, 2$, respectively [25],
ϵ_π : pion detection efficiency =0.6 (solid angle coverage of CDC and CDH),
ϵ_n : neutron detection efficiency ~ 0.05 for neutrons over 5 MeV kinetic energy assuming 1 MeV*ee* detection threshold,
ϵ_{DAQ} : DAQ live time rate = 0.7,
ϵ_{ANA} : Analysis efficiency = 0.9,

and we finally obtain

$$Y_1 = 7.9 \times 10^4, Y_2 = 1.1 \times 10^5. \quad (14)$$

This statistics is more than two orders higher than that of $\Sigma^-\pi^+t$, 652 events [13], and we aim to investigate the nature of $\Lambda(1405)$ with this high-statistics and high-resolution data with the most simple reaction.

6 Expected spectra and sensitivity

On the top of figure 11, we present the expected spectra from two hypotheses, assuming the realistic mass resolution and stopped K^- number as described in Secs. 4.3 and 5, respectively. As found in the top figure, the expected spectra reproduce the theoretical calculation excellently due to the perfect mass resolution at the high-mass region and statistics of ~ 10^5 events, and two scenarios, $\Lambda(1405)$ and $\Lambda(1420)$, can be distinctly discriminated as the result, as quantitatively shown in the bottom of figure 11. This high-statistics and high-precision data will allow us to determine the mass and the width of the Λ^* very precisely, even in the case that the measured spectrum is deviated from the both model calculations to update the PDG value of the mass and the width.

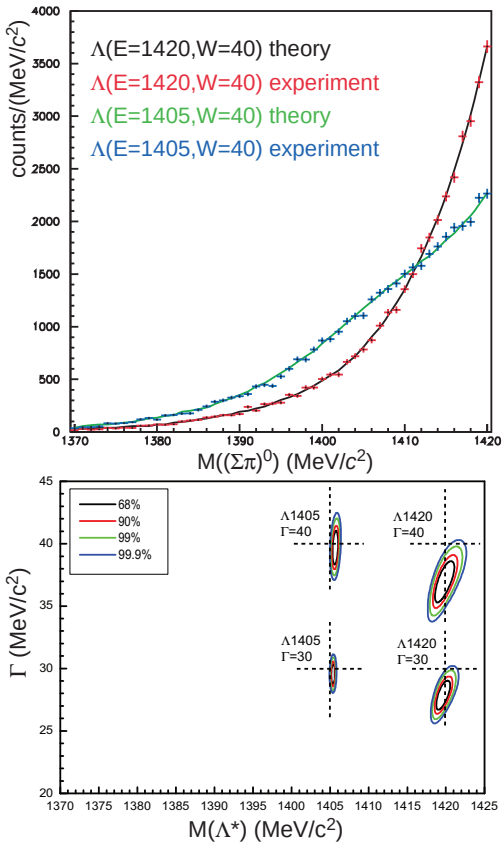

Fig. 11. Top: Simulated $M_{(\Sigma\pi)^0}$ spectra from the two different scenarios of $\Lambda(1405)$ (7.4×10^4 events, blue) and $\Lambda(1420)$ (1.0×10^5 events, red) are drawn with error bars, and overlaid on the theoretical calculation (green and blue real lines, for $\Lambda(1405)$ and $\Lambda(1420)$, respectively). In both calculations, the width of 40 MeV is assumed. Bottom: Expected sensitivity of the mass and the width of Λ^* for various cases, assuming ~40% of expected statistics [14].

7 Summary and conclusion

In order to give an answer to the currently debated hot topics on the structure of the Λ^* resonance, we have discussed $\bar{K}N \to \Sigma\pi$ reaction and related observables under the coupled channel scheme in a way available for both single- and double-pole models of Λ^*. We conclude that the spectrum

shape depends only on the first or single pole position, and hence the reaction is the most relevant to judge two counter hypothesis.

According to the theoretical consideration, we have proposed a new experiment to measure the $(\Sigma\pi)^0$ mass spectra by means of the stopped K^- reaction on liquid deuterium at the J-PARC K1.8BR beamline with the E15/E17 experimental devices, so as to obtain new high-precision and high-statistics data to determine experimentally the exact first/single pole position. As the result of studies from various angles including Monte-Carlo simulations taking realistic experimental conditions into account, we expect the proposal to have sufficient sensitivity to resolve the controversial situation. The resolution will lead the final answer of the yet unresolved problem of $\bar{K}N$ interaction and $\bar{K}$-nuclei.

References

1. M. H. Alston *et al.*, Phys. Rev. Lett. **6** (1961) 698.
2. M. Iwasaki *et al.*, Phys. Rev. Lett. **78** (1997) 3067.
3. A. D. Martin, Nucl. Phys. **B179** (1981) 33.
4. Y. Akaishi and T. Yamazaki, Phys. Rev. C **65** (2002) 044005.
5. T. Yamazaki and Y. Akaishi, Phys. Lett. B **535** (2002) 70.
6. V. K. Magas, E. Oset, and A. Ramos, Phys. Rev. Lett. **95** (2005) 052301.
7. T. Hyodo and W. Weise, Phys. Rev. C **77** (2008) 035204.
8. R. H. Dalitz and A. Deloff, J. Phys. G **17** (1991) 289.
9. R. J. Hemingway, Nucl. Phys. **B253** (1985) 742.
10. D. Jido, E. Oset, and T. Sekihara, Eur. Phys. J. **A42** (2009) 257.
11. H. Noumi *et. al*, Proposal for J-PARC 50 GeV Proton Synchrotron,
" *Spectroscopic study of hyperon resonances below $\bar{K}N$ threshold via the (K^-, n) reaction on deuteron* " (J-PARC P31), 2009.
12. J. Esmaili, Y. Akaishi, and T. Yamazaki, ArXiv:0906.0505.
13. B. Riley *et al.*, Phys. Rev. D **11** (1975) 3065.
14. J. Esmaili, Y. Akaishi, and T. Yamazaki, ArXiv:0909.2573.
15. J. Revai and N. V. Shevchenco, Phys. Rev. C **79** (2009) 035202.
16. T. Suzuki *et al.*, Phys. Rev. C **76** (2007) 068202.
17. R.S. Hayano, H. Outa *et. al*, Proposal for J-PARC 50 GeV Proton Synchrotron,
" *Precision spectroscopy of Kaonic Helium 3 $3d \rightarrow 2p$ X-rays*" (J-PARC E17), 2006.
18. M. Iio for J-PARC E17 collaboration, in this volume.
19. Y. Fujiwara for J-PARC E17 collaboration, in this volume.
20. T. Suzuki *et. al*, Proposal for J-PARC 50 GeV Proton Synchrotron,
" *The investigation of $\Lambda(1405)$ state via the $d(K^-_{stopped}, n)(\Sigma\pi)^0$ reaction*" (J-PARC P30), 2009.
21. M. Iwasaki, T. Nagae *et. al*, Proposal for J-PARC 50 GeV Proton Synchrotron,
" *A search for deeply-bound kaonic nuclear states by in-flight ^{3}He(K^-, n) reaction*" (J-PARC E15), 2006.
22. K. Tsukada for J-PARC E15 collaboration, in this volume.
23. R. C. Byrd *et al.*, Nucl. Instrum. Methods **A313** (1992) 437.
24. H. Yim *et al.*, submitted to Phys. Lett. B.
25. C. Vander Velde-Wilquet *et al.*, NUOVO CIM. **A39** (1977) 538.